NANO LETTERS

Letter

pubs.acs.org/NanoLett

Stabilization of Ferromagnetic Order in $La_{0.7}Sr_{0.3}MnO_3$–$SrRuO_3$ Superlattices

M. Ziese,*[,†] F. Bern,[†] E. Pippel,[‡] D. Hesse,[‡] and I. Vrejoiu*[,‡,§]

[†]Division of Superconductivity and Magnetism, University of Leipzig, D-04103 Leipzig, Germany

[‡]Max Planck Institute of Microstructure Physics, D-06120 Halle, Germany

ABSTRACT: The study of spatially confined complex oxides is of wide interest, since correlated electrons at interfaces might form exotic phases. Here $La_{0.7}Sr_{0.3}MnO_3/SrRuO_3$ superlattices with coherently grown interfaces were studied by structural techniques, magnetization, and magnetotransport measurements. Magnetization measurements showed that ferromagnetic order in ultrathin $La_{0.7}Sr_{0.3}MnO_3$ layers is stabilized in the superlattices down to layer thicknesses of at least two unit cells. This stabilization is destroyed, if the ferromagnetic layers are separated by two unit cell thick $SrTiO_3$ layers. The resistivity of the superlattices showed metallic behavior and was dominated by the conducting $SrRuO_3$ layers, the off-diagonal resistivity showed an anomalous Hall effect from both $SrRuO_3$ and $La_{0.7}Sr_{0.3}MnO_3$ layers. This shows that the $La_{0.7}Sr_{0.3}MnO_3$ layers are not only ferromagnetic but also highly conducting; probably a conducting hole gas is induced at the interfaces that stabilizes the ferromagnetic order. This result opens up an alternative route for the fabrication of two-dimensional systems with long-range ferromagnetic order.

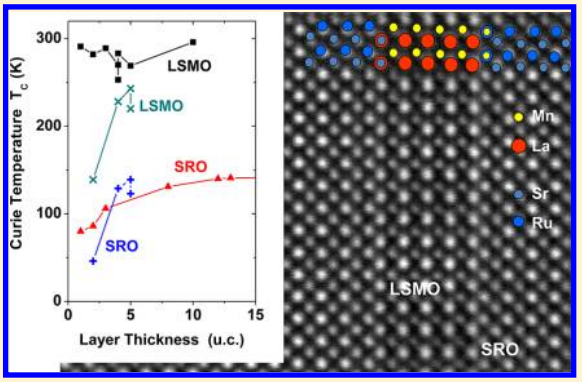

KEYWORDS: *Oxide interfaces, $La_{0.7}Sr_{0.3}MnO_3$, $SrRuO_3$, magnetotransport, interfacial electron gas*

It is a common observation that the Curie temperature of ferromagnetic films decreases with decreasing film thickness. This might be related to general physical concepts such as finite size scaling,[1] to material-specific intrinsic properties such as electronic phase separation,[2] or to growth characteristics and microstructure.[3] In this context ferromagnetic oxide films were intensely studied in recent years, since these promised to yield new insights into spatially confined strongly correlated systems. The strong coupling between electron, spin, orbital, and phonon degrees of freedom in the colossal magnetoresistance manganites leads to the formation of insulating antiferromagnetic states in thin layers of originally metallic ferromagnetic compounds.[4,5] On a phenomenological basis, this can be either understood by orbital ordering and the weakening of the double exchange mechanism in a particular direction in a strained Manganite lattice[5−7] or by interfacially driven electronic phase separation.[8,9]

The metal−insulator transition observed in ultrathin manganite films with optimal doping depends on the substrate material,[4,10,11] probably due to variations in the strain state, but also on the thin film deposition conditions,[4,11,12] possibly due to the growth mode, defect type, and defect density. Although there is some variability in the critical thickness for entering the insulating region, this has not been observed to be smaller than 8 unit cells.[12] In $SrTiO_3$(STO)/$La_{0.7}Sr_{0.3}MnO_3$(LSMO) superlattices (SLs) also a strong suppression of the Curie temperature (T_C) was observed,[13,14] but recently a T_C stabilization was reported in optimized samples.[15] It is well-known that LSMO and $SrRuO_3$ (SRO) show an antiferromagnetic interfacial exchange coupling[16−19] that is related to the direct Mn−Ru coupling across the interface.[19,20] In this work, the implications of the interlayer exchange coupling on the ferromagnetism of the LSMO layers is explored. It is found that the Curie temperature of the LSMO layers can be stabilized near room temperature values down to a layer thickness of at least 2 unit cells, whereas the T_C of the SRO layers shows a typical decrease with decreasing layer thickness.

Since the stabilization of the Curie temperature is related to the presence of LSMO-SRO interfaces, it might be related to the presence of an electron gas formed at that interface. It is known that at the interface between two complex oxides charge carriers may be confined leading to the emergence of strong correlation and collective effects. In the system $SrTiO_3/LaAlO_3$, it was recently shown that ferromagnetism appears at the interface, although the forming oxides are not ferromagnetic.[21] Furthermore, in this system the coexistence of ferromagnetism and superconductivity, presumably carried by a two-dimensional (2D), albeit phase-separated, electron gas, was reported.[22,23] The mechanism leading to ferromagnetism in this 2D system[24,25] has not yet been clarified. Moreover, there is an ongoing debate whether the $SrTiO_3/LaAlO_3$ interface is a valid model system for the test of fundamental theories, since

Received: May 24, 2012
Revised: July 4, 2012
Published: July 9, 2012

   dx.doi.org/10.1021/nl301963a | *Nano Lett.* 2012, 12, 4276−4281

there is extensive experimental evidence for diffusional mixing and related doping effects at this interface.[26] Therefore we believe that the observation of similar effects at other oxide interfaces will play a crucial role for a further understanding of confined correlated electron gases.

Films, bilayers, and superlattices (SLs) were fabricated by pulsed laser deposition from stoichiometric polycrystalline targets onto vicinal $SrTiO_3$ (001) substrates with uniform TiO_2−termination and a terrace morphology with typically 150−400 nm terrace width. Substrate temperature was 650 °C and oxygen partial pressure 0.14 mbar. All samples grew in the step-flow growth mode. For this study, LSMO and SRO single films, LSMO/SRO SLs and a LSMO/SRO bilayer, LSMO/SRO SLs with $SrTiO_3$ interlayers and a LSMO/STO SL were selected, see Table 1. Samples are in general denoted by the individual layer thicknesses expressed in unit cells (u.c.).

Table 1. Samples Measured in This Work with Layer Thicknesses (in u.c.) and Curie Temperatures[a]

sample	SRO film	$T_{C,SRO}$	
0/12	$[0/12]_1$	145 K	
sample	LSMO film		$T_{C,LSMO}$
38/0	$[38/0]_1$		330 K
10/0	$[10/0]_1$		296 K
4/0	$[4/0]_1$		
sample	$[LSMO/SRO]_n$	$T_{C,SRO}$	$T_{C,LSMO}$
4/20	$[4/20]_{15}$	142 K	283 K
4/12	$[4/12]_{15}$	140 K	253 K
4/8	$[4/8]_{15}$	131 K	270 K
3/3	$[3/3]_{15}$	106 K	289 K
2/2	$[2/2]_{15}$	86 K	282 K
1/1	$[1/1]_{22}$	80 K	291 K
5/13	$[5/13]_1$	139 K	269 K
sample	$[LSMO/STO/SRO/STO]_n$	$T_{C,SRO}$	$T_{C,LSMO}$
5/4/13/4	$[5/4/13/4]_{10}$	139 K	243 K
4/2/13/2	$[4/2/13/2]_{15}$	123 K	228 K
5/2/8/2	$[5/2/8/2]_{15}$	129 K	217 K
2/2/2/2	$[2/2/2/2]_{15}$	46 K	139 K
3/3S	$[3/3/0/0]_{15}$		35 K

[a]Subscripts indicate the number of repetitions.

The microstructure of the SLs was investigated by high-angle annular dark field−scanning transmission electron microscopy (HAADF-STEM) in a TITAN 80−300 FEI microscope; energy dispersive X-ray spectroscopy (EDX) as well as electron energy loss spectroscopy (EELS) were performed with atomic resolution in order to probe the atomic structure of the interfaces and to check for chemical interdiffusion. Magnetization measurements were performed in a Quantum Design MPMS-7 SQUID magnetometer. The resistance and Hall effect were measured in van-der-Pauw geometry. Longitudinal and Hall resistivity were calculated using the conducting SRO layer thickness only, since SRO films were shown to be metallic down to a thickness of 2 unit cells.[27] The Curie temperatures T_C were determined from magnetization and resistivity measurements. We have used a stringent criterion, namely the maxima/minima in the derivatives to determine T_C.

HAADF-STEM micrographs of SLs 4/8 and 2/2 are shown in Figure 1. The interfaces between the LSMO and SRO layers were coherent, see also refs 19 and 28. There is Mn/Ru intermixing on the length scale of half a unit cell for the SLs

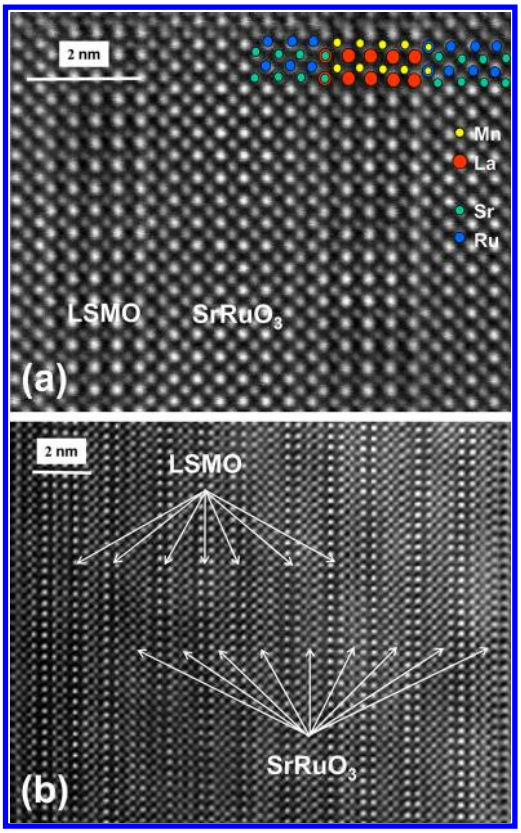

Figure 1. (a) HAADF-STEM micrograph of sample SL 4/8 showing the interfaces between two 4 u.c. thick LSMO layers and the adjacent 8 u.c. thick SRO layers. The colored circles indicate the cations as determined from the Z-contrast. (b) HAADF-STEM micrograph of sample SL 2/2 showing a sequence of 2 u.c. thick LSMO and SRO layers. Note the different sizes of the scale bars.

with layers thinner than 4 u.c.[19,28] This is indicated in Figure 1a by the colored circles: at the right interface of the LSMO layer intermixing between Mn and Ru is indicated, and at the left interface the rare earth sites might be occupied by La or Sr. Apart from SL 1/1, measurements in various areas showed that the layer thicknesses were uniform over the sample; SL 1/1 consisted of 1/1, 1/2, and 2/1 areas.

The magnetic moment of selected samples is shown in Figures 2 and 3a as a function of temperature. The measured magnetic moment was converted to the equivalent moment per Mn ion, since this allows for a quick overview of the LSMO layer contribution. Most samples were not fully saturated in a magnetic field of 0.1 T, but the application of higher magnetic fields leads to a broadening of the magnetic transitions, so the 0.1 T data were selected for a compromise. In Figure 2a, the magnetic moments of the 10 and the 4 u.c. thick film as well as the LSMO/STO SL are compared. Whereas the 10 u.c. thick LSMO film is clearly ferromagnetic with a Curie temperature close to room temperature, the 4 u.c. thick LSMO is not ferromagnetic, and the ferromagnetism in the LSMO/STO SL is rather weak with a low T_C and a small magnetic moment per Mn ion. This is in agreement with literature data.[4,11−14] The critical thickness for the onset of ferromagnetism in thin LSMO films on STO is therefore larger than 4 u.c. In 5/5 LSMO/STO SLs, T_C reaches 220 K only when grown at low O_2 partial pressure.[15] However, in this case STO interlayers may be semiconducting due to slight oxygen deficiency.

dx.doi.org/10.1021/nl301963a | Nano Lett. 2012, 12, 4276−4281

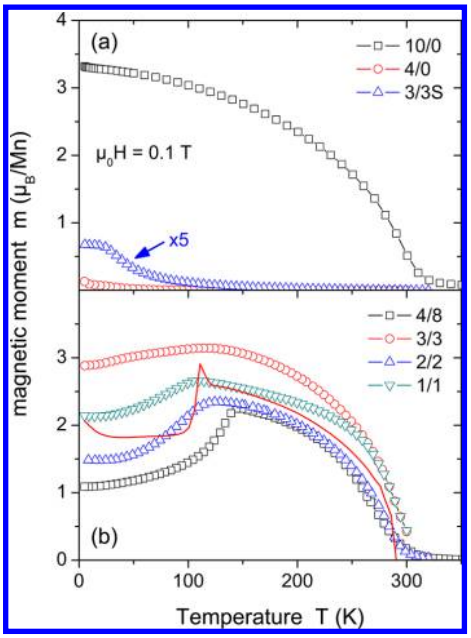

Figure 2. (a) Magnetization of the 10 u.c. and 4 u.c. thick LSMO films as well as of the LSMO/STO SL 3/3S. (b) Magnetization of LSMO/SRO SLs. The solid line in (b) is the remanent magnetization of SL 3/3.

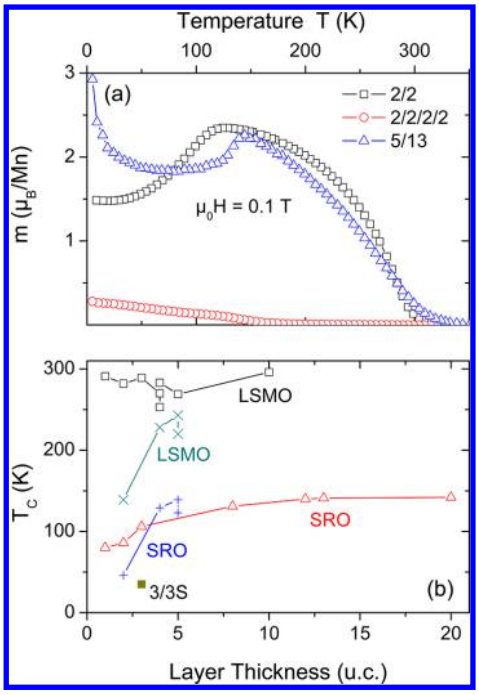

Figure 3. (a) Magnetization of the LSMO/SRO SL 2/2 in comparison to the corresponding LSMO/STO/SRO/STO SL 2/2/2/2 as well as the LSMO/SRO bilayer 5/13. (b) Curie temperatures T_C of LSMO and SRO layers as a function of LSMO and SRO layer thickness, respectively: LSMO (□) and SRO (Δ) in LSMO/SRO SLs, LSMO (×) and SRO (+) in LSMO/STO/SRO/STO SLs.

Figure 2b shows the magnetic moment of the LSMO/SRO SLs with the smallest layer thicknesses. All these SLs showed clear ferromagnetic transitions near room temperature, sizable fractions of the spin-only moment of LSMO of 3.7 μ_B/Mn, and the antiferromagnetic interlayer coupling between LSMO and SRO layers below the T_C of the SRO layers.[19] This is a central result of this work: in LSMO/SRO SLs the ferromagnetic order in the LSMO layers is stabilized with T_C values far above the T_C of the SRO layers. Since the transitions of the SRO layers were broadened for SLs 3/3, 2/2, and 1/1, the T_C of the SRO layers of these samples was determined from the sharp jump in the remanent magnetization. This is illustrated in Figure 2b. Whereas the magnetic moment of sample 3/3 measured in 0.1 T does not show a clear indication of the ferromagnetic transition of the SRO layers, the remanent magnetization, measured on warming after cooling the SL in 0.1 T and setting the field to zero at 5 K, shows a sharp jump at the T_C of the SRO layers.

The stabilization of the ferromagnetic order in the LSMO/SRO SLs might be due to various factors such as a RKKY-like coupling of the LSMO layers across the conducting SRO layers, the magnetic coupling between Mn and Ru ions at the interface, charge transfer from SRO to LSMO layers or a reduction in the density of growth defects in the LSMO layers due to the modified epitaxy conditions. The first two factors were directly probed experimentally. Figure 3a shows a comparison of the magnetic moment of the LSMO/SRO SL 2/2 with the LSMO/SRO bilayer 5/13 and with the LSMO/STO/SRO/STO SL 2/2/2/2 in which adjacent LSMO and SRO layers were separated by 2 u.c. thick STO layers. Since the bilayer also shows the T_C stabilization of the LSMO layer, a RKKY mechanism does not seem to play a major role for this effect. On the other hand, the insertion of STO interlayers does significantly reduce the magnetic moment and the T_C, indicating that either the direct Mn−Ru coupling or a charge transfer mechanism might indeed play a vital role in the stabilization of the ferromagnetic order. In general the contact to a conducting layer does not restore ferromagnetism in LSMO, see the strong T_C decrease in LSMO films in contact with Au.[29] Possible Ru-doping due to intermixing does only lead to a modest T_C-increase[30] and cannot explain the restoration of ferromagnetism in ultrathin LSMO layers.

The Curie temperatures of the LSMO and SRO layers are shown in Figure 3b as a function of the respective layer thicknesses. The data fall into two groups. The series of LSMO/SRO SLs shows a stabilization of the ferromagnetic order in the LSMO layers down to at least a LSMO layer thickness of 2 u.c.; there is actually a trend for the Curie temperature to increase for decreasing layer thicknesses below 5 u.c. However, there is also a considerable sample-to-sample variation as is evident from the data points at 4 u.c. On the other hand, the SRO layer T_C's in this LSMO/SRO series decrease gradually with decreasing SRO layer thickness as also found in SRO films[27] and SRO/STO SLs.[31] This is the conventional behavior of the Curie temperature in thin ferromagnetic films. In the series of LSMO/STO/SRO/STO SLs, the Curie temperatures of both LSMO and SRO layers decrease with decreasing layer thickness and rather sharply so below a thickness of 4 u.c. This is similar to the behavior commonly observed in LSMO/STO and SRO/STO SLs; with the maximum slope criterion for T_C a 5 u.c. thick LSMO layer in a LSMO/STO/SRO/STO SL had a T_C of about 230 K, see Figure 3b, which is in agreement with the value obtained for optimized LSMO/STO SLs.[15] A central finding of the present work is the bifurcation of the LSMO T_C curves in Figure 3b below a layer thickness of 5 u.c. that clearly proves the stabilization of the ferromagnetic order in the LSMO layers of the LSMO/SRO SLs.

dx.doi.org/10.1021/nl301963a | Nano Lett. 2012, 12, 4276−4281

The results presented above have two important implications. The data clearly show that the undisturbed LSMO/SRO interface is essential for the T_C stabilization. It is unlikely that the T_C of the LSMO layers is stabilized by the antiferromagnetic Mn−Ru coupling, since the T_C of the SRO layers is far too low. Therefore the ferromagnetism is induced in the LSMO layers probably by charge transfer from the SRO layers,[32] thus forming a charge carrier gas. Further, in the context of finite size scaling the results are important, since the LSMO/SRO SLs can be viewed as a heterogeneous system with two magnetic components; whereas the SRO layers show conventional finite size scaling effects, the T_C of the LSMO layers does not show finite size scaling down to a thickness of at least 2 u.c. This corroborates that the mechanism leading to ferromagnetism in the LSMO layers is exceptional.

In order to highlight the properties of the LSMO layers further, we have studied the resistivity as shown in Figure 4.

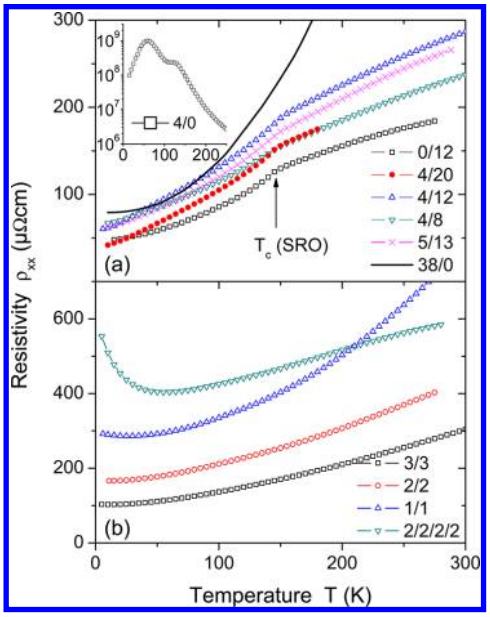

Figure 4. Zero-field resistivity as a function of temperature. The inset shows the resistivity of a 4 u.c. thick LSMO single film. Axis units of the inset are the same as for the main panel.

Apart from the 4 u.c. thick LSMO film all samples showed metallic behavior. The 4 u.c. thick LSMO film was practically insulating with a resistivity enhanced by several orders of magnitude compared to the other samples.[4,12] Compared to the single SRO film the resistivity of the SLs is enhanced, presumably due to the increasing importance of interfacial scattering. The similarity of the resistivity of the SRO film, the bilayer 5/13, and the SLs 4/20, 4/12 and 4/8 with the bulk SRO resistivity[33] indicate that the conduction in these samples was dominated by the SRO layers.

The contribution of the LSMO layers to the transport properties can be studied using Hall effect measurements. The Hall resistivity is expected to follow[34] $\rho_{yx} = R_H B + R_A M$ with the ordinary R_H and anomalous R_A Hall constants; M denotes the magnetization component perpendicular to the layers. The Hall resistivity of the SRO and LSMO films as well as SLs 2/2 and 2/2/2/2 is shown in Figure 5 at 10 and 250 K. At 10 K samples, 0/12 and 2/2/2/2 showed a negative high-field slope, since electron conduction prevails in SRO. The anomalous Hall resistivity was either negative or positive, since the SRO layers

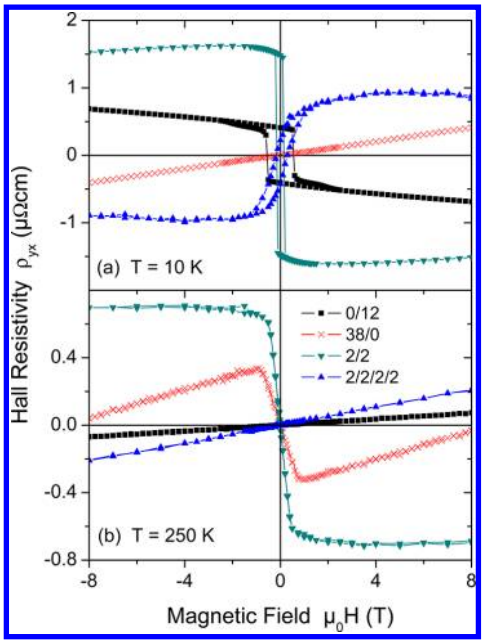

Figure 5. Hall resistivity at (a) 10 K and (b) 250 K as a function of magnetic field. Data for sample 2/2/2/2 were measured at 5 and 150 K.

have either orthorhombic (0/12) or tetragonal (2/2/2/2)[35] symmetry. The LSMO film 38/0 showed only an ordinary Hall effect at 10 K indicating hole conduction; the anomalous Hall contribution vanishes in LSMO at low temperatures, see, for example, ref 36. The large negative anomalous Hall effect and the holelike high-field slope of SL 2/2 at 10 K were unexpected and are a central result of the Hall-effect measurements. Figure 5b further shows that at 250 K SL 2/2 had a clear ferromagnetic contribution from the anomalous Hall effect, although the conducting SRO layers were already in the paramagnetic regime and the LSMO layers were expected to be insulating and antiferromagnetic for this small layer thickness.[4,12] This proves that the LSMO layers in the LSMO/SRO SLs are not only ferromagnetic but also conducting. The ferromagnetic Hall-effect contribution depended on the direct contact between LSMO and SRO layers, since it could be switched off by the insertion of STO interlayers (sample 2/2/2/2). Despite electron conduction, the Hall effect of the SRO film 0/12 and the SL 2/2/2/2 is positive in the paramagnetic regime due to a strong positive contribution from the anomalous Hall effect.

The unexpected ferromagnetic anomalous Hall effect contribution is shown for the bilayer 5/13 and the SL 2/2 for various temperatures in Figure 6. The bilayer has a comparatively thick SRO layer that clearly dominates the Hall effect at low temperatures. The intricate behavior at 140 K with magnetization reversal in low magnetic fields is due to the exchange coupling of the SRO and LSMO layers. At 160 K and above a clear ferromagnetic Hall effect contribution emerges that is attributed to the LSMO layer. SL 2/2 had a ferromagnetic contribution to the Hall effect up to the highest measured temperature of 250 K. The temperature dependence of the anomalous Hall effect in samples 3/3, 2/2 and 1/1 strikingly differs from that of LSMO and SRO.

One would be tempted to model the Hall resistivity by LSMO and SRO layers conducting in parallel. In case of bilayer 5/13 and SLs 4/20, 4/12, and 4/8, this is possible at 200 K and

dx.doi.org/10.1021/nl301963a | Nano Lett. 2012, 12, 4276−4281

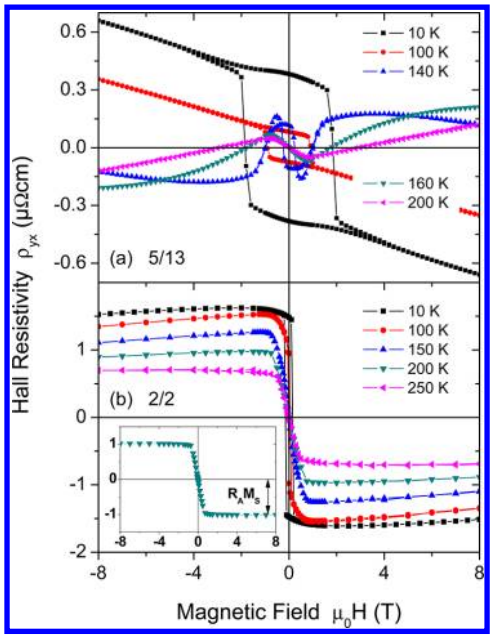

Figure 6. Hall resistivity of (a) bilayer 5/13 and (b) SL 2/2 as a function of magnetic field for various temperatures. The inset in (b) shows the 200 K data after subtraction of the ordinary Hall effect. The determination of the anomalous Hall effect $R_A M_S$ is indicated.

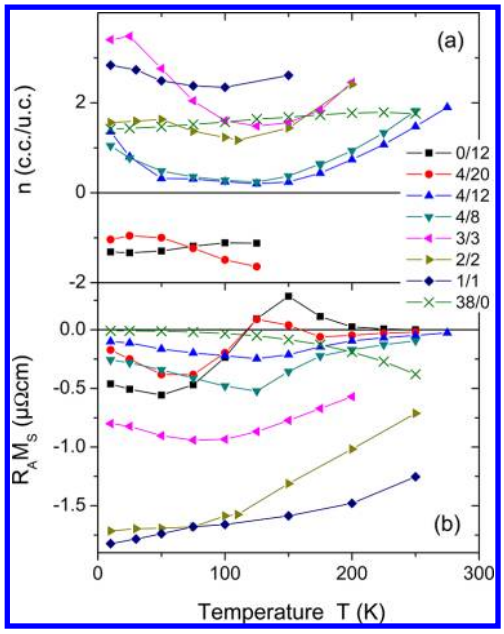

Figure 7. (a) Carrier concentration per unit cell as a function of temperature. Positive (negative) values indicate hole (electron) conduction. (b) Saturation anomalous Hall effect $R_A M_S$ as a function of temperature.

above, when a resistivity of the LSMO layers is assumed that is at least five times smaller than the resistivity of the single SRO film. In the case of SLs 3/3, 2/2, and 1/1, such a modeling is not possible, since the temperature dependence of the anomalous Hall component does not agree with that of the single SRO and LSMO films. This shows that the anomalous Hall effect contribution measured in the SLs above the Curie temperature of the SRO layers arises from highly conducting, ferromagnetic layers. Since the insertion of 2 u.c. thick $SrTiO_3$ interlayers destroyed this conducting state, it is very probably related to the LSMO-SRO interface.

The Hall effect data were further characterized by determining the carrier concentration from the high field slope as well as the saturation anomalous Hall effect $R_A M_S$ from the high-field data after subtraction of the ordinary Hall contribution. The carrier concentration per unit cell calculated within a one-band model is shown in Figure 7a. In agreement with literature values[36,37] SRO shows electron and LSMO hole conduction. With decreasing thickness of the SRO layers the carrier concentration of the SLs evolves from electron to hole conduction. This indicates the formation of a hole gas within the LSMO layers contributing to the overall carrier concentration. The temperature dependence of the Hall effect of orthorhombic SRO is known to be rather complex[38] and explains the data for the samples with thicker SRO films. However, the weak temperature dependence and comparatively large value of the anomalous Hall contribution of samples 3/3, 2/2 and 1/1 is unexpected. This we interpret as the Hall effect contribution from the interfacial hole gas that emerges more and more clearly for thinner layers.

The central observation of this work is the existence of highly conducting, ferromagnetic regions at the LSMO-SRO interface. This result might be understood by the fact that the chemical potential μ in a double exchange system varies with the magnetization M, $\delta\mu/W \propto M^2$, where W is the bandwidth of LSMO.[32] STO layers were found to be hole-donating, thus driving the near-interface regions of LSMO toward the overdoped antiferromagnetic state.[39] Our findings indicate that SRO is electron-donating, such that the ferromagnetic conducting state is stabilized in the LSMO layers. This scenario would explain both the existence of conducting interfaces as well as their ferromagnetic order. A RKKY-like coupling of LSMO layers across SRO layers seems to play a minor role, since the bilayer 5/13 also shows the formation of a hole gas. The width of the induced hole gas layer in these samples is difficult to estimate; however, since this effect is emerging in the LSMO/SRO SLs, it is likely to be located close to the interfaces. At the $CaRuO_3/CaMnO_3$ interface,[40] a similar electron-leakage effect with a penetration depth of 2 u.c.[41] was found.

In summary, the study of the magnetization and Hall effect of LSMO/SRO superlattices showed the existence of a ferromagnetic hole gas located at the LSMO/SRO interface. This has a conductivity comparable to that of SRO and a large carrier density characteristic of metals. This hole gas is shunted by the metallic SRO layers, but can be observed by Hall resistivity measurements. We believe that our results have opened up an alternative route for the fabrication of two-dimensional spintronic devices.

AUTHOR INFORMATION

Corresponding Author

*E-mail: (M.Z,) ziese@physik.uni-leipzig.de; (I.V.) I.Vrejoiu@fkf.mpg.de.

Present Address

[§]Max Planck Institute for Solid State Research, D-70569 Stuttgart, Germany.

Notes

The authors declare no competing financial interest.

■ ACKNOWLEDGMENTS

This work was supported by the DFG within SFB 762 "Functionality of Oxide Interfaces"; F.B. is member of the Leipzig School of Natural Sciences "BuildMoNa". We thank P. Esquinazi for a critical reading of the manuscript.

■ REFERENCES

(1) Huang, F.; Kief, M. T.; Mankey, G. J.; Willis, R. F. *Phys. Rev. B* **1994**, *49*, 3962.
(2) Dagotto, E.; Hotta, T.; Moreo, A. *Phys. Rep.* **2001**, *344*, 1.
(3) Xie, C.; Budnick, J. I.; Wells, B. O.; Woicik, J. C. *Appl. Phys. Lett.* **2007**, *91*, 172509.
(4) Konishi, Y.; Fang, Z.; Izumi, M.; Manako, T.; Kasai, M.; Kuwahara, H.; Kawasaki, M.; Terakura, K.; Tokura, Y. *J. Phys. Soc. Jpn.* **1999**, *68*, 3790.
(5) Fang, Z.; Solovyev, I. V.; Terakura, K. *Phys. Rev. Lett.* **2000**, *84*, 3169.
(6) Tebano, A.; Aruta, C.; Sanna, S.; Medaglia, P. G.; Balestrino, G.; Sidorenko, A. A.; Renzi, R. D.; Ghiringhelli, G.; Braicovich, L.; Bisogni, V.; Brookes, N. B. *Phys. Rev. Lett.* **2008**, *100*, 137401.
(7) Baena, A.; Brey, L.; Calderón, M. J. *Phys. Rev. B* **2011**, *83*, 064424.
(8) Jo, M.-H.; Mathur, N. D.; Todd, N. K.; Blamire, M. G. *Phys. Rev. B* **2000**, *61*, R14905.
(9) Bibes, M.; Balcells, L.; Valencia, S.; Fontcuberta, J.; Wojcik, M.; Jedryka, E.; Nadolski, S. *Phys. Rev. Lett.* **2001**, *87*, 067210.
(10) Ziese, M.; Semmelhack, H. C.; Han, K. H.; Sena, S. P.; Blythe, H. J. *J. Appl. Phys.* **2002**, *91*, 9930.
(11) Ziese, M.; Semmelhack, H. C.; Han, K.-H. *Phys. Rev. B* **2003**, *68*, 134444.
(12) Huijben, M.; Martin, L. W.; Chu, Y.-H.; Holcomb, M. B.; Yu, P.; Rijnders, G.; Blank, D. H. A.; Ramesh, R. *Phys. Rev. B* **2008**, *78*, 094413.
(13) Ma, J. X.; Liu, X. F.; Lin, T.; Gao, G. Y.; Zhang, J. P.; Wu, W. B.; Li, X. G.; Shi, J. *Phys. Rev. B* **2009**, *79*, 174424.
(14) Dekker, M. C.; Herklotz, A.; Schultz, L.; Reibold, M.; Vogel, K.; Biegalski, M. D.; Christen, H. M.; Dörr, K. *Phys. Rev. B* **2011**, *84*, 054463.
(15) Kourkoutis, L. F.; Song, J. H.; Hwang, H. Y.; Muller, D. A. *Proc. Natl. Acad. Sci. U.S.A.* **2010**, *107*, 11682.
(16) Ke, X.; Rzchowski, M. S.; Belenky, L. J.; Eom, C. B. *Appl. Phys. Lett.* **2004**, *84*, 5458.
(17) Ke, X.; Belenky, L. J.; Eom, C. B.; Rzchowski, M. S. *J. Appl. Phys.* **2005**, *97*, 10K115.
(18) Padhan, P.; Prellier, W.; Budhani, R. C. *Appl. Phys. Lett.* **2006**, *88*, 192509.
(19) Ziese, M.; Vrejoiu, I.; Pippel, E.; Esquinazi, P.; Hesse, D.; Etz, C.; Henk, J.; Ernst, A.; Maznichenko, I. V.; Hergert, W.; Mertig, I. *Phys. Rev. Lett.* **2010**, *104*, 167203.
(20) Lee, Y.; Caes, B.; Harmon, B. Role of Oxygen 2p states for antiferromagnetic interfacial coupling and positive exchange bias of ferromagnetic LSMO/SRO bilayers. *J. Alloys Compd.* **2008**, *450*, 1−6.
(21) Brinkman, A.; Huijben, M.; van Zalk, M.; Huijben, J.; Zeitler, U.; Maan, J. C.; van der Wiel, W. G.; Rijnders, G.; Blank, D. H. A.; Hilgenkamp, H. *Nat. Mater.* **2007**, *6*, 493.
(22) Ariando,; Wang, X.; Baskaran, G.; Liu, Z. Q.; Huijben, J.; Yi, J. B.; Annadi, A.; Barman, A. R.; Rusydi, A.; Dhar, S.; Feng, Y. P.; Ding, J.; Hilgenkamp, H.; Venkatesan, T. *Nat. Commun.s* **2011**, *2*, 288.
(23) Dikin, D. A.; Mehta, M.; Bark, C. W.; Folkman, C. M.; Eom, C. B.; Chandrasekhar, V. *Phys. Rev. Lett.* **2011**, *107*, 056802.
(24) Okamoto, S.; Millis, A. J.; Spaldin, N. A. *Phys. Rev. Lett.* **2006**, *97*, 056802.
(25) Pentcheva, R.; Pickett, W. E. *Phys. Rev. Lett.* **2007**, *99*, 016802.
(26) Chambers, S. A.; Engelhard, M. H.; Shutthanandan, V.; Zhu, Z.; Droubay, T. C.; Qiao, L.; Sushko, P. V.; Feng, T.; Lee, H. D.; Gustafsson, T.; Garfunkel, E.; Shah, A. B.; Zuo, J.-M.; Ramasse, Q. M. *Surf. Sci. Rep.* **2010**, *65*, 317.
(27) Chang, Y. J.; Kim, C. H.; Phark, S.-H.; Kim, Y. S.; Yu, J.; Noh, T. W. *Phys. Rev. Lett.* **2009**, *103*, 057201.
(28) Hillebrand, R.; Pippel, E.; Hesse, D.; Vrejoiu, I. *Phys. Status Solidi A* **2011**, *208*, 2144.
(29) Brivio, S.; Magen, C.; Sidorenko, A. A.; Petti, D.; Cantoni, M.; Finazzi, M.; Ciccacci, F.; De Renzi, R.; Varela, M.; Picozzi, S.; Bertacco, R. *Phys. Rev. B* **2010**, *81*, 094410.
(30) Yamada, H.; Kawasaki, M.; Tokura, Y. *Appl. Phys. Lett.* **2005**, *86*, 192505.
(31) Izumi, M.; Nakazawa, K.; Bando, Y. *J. Phys. Soc. Jpn.* **1998**, *67*, 651.
(32) Furukawa, N. *J. Phys. Soc. Jpn.* **1997**, *66*, 2523.
(33) Cao, G.; McCall, S.; Shepard, M.; Crow, J. E.; Guertin, R. P. *Phys. Rev. B* **1997**, *56*, 321−329.
(34) Nagaosa, N.; Sinova, J.; Onoda, S.; MacDonald, A. H.; Ong, N. P. *Rev. Mod. Phys.* **2010**, *82*, 1539.
(35) Ziese, M.; Vrejoiu, I. *Phys. Rev. B* **2011**, *84*, 104413.
(36) Ziese, M.; Srinitiwarawong, C. *Europhys. Lett.* **1999**, *45*, 256.
(37) Kats, Y.; Genish, I.; Klein, L.; Reiner, J. W.; Beasley, M. R. *Phys. Rev. B* **2004**, *70*, 180407(R).
(38) Mathieu, R.; Asamitsu, A.; Yamada, H.; Takahashi, K. S.; Kawasaki, M.; Fang, Z.; Nagaosa, N.; Tokura, Y. *Phys. Rev. Lett.* **2004**, *93*, 016602.
(39) Yamada, H.; Ogawa, Y.; Ishii, Y.; Sato, H.; Kawasaki, M.; Akoh, H.; Tokura, Y. *Science* **2004**, *305*, 646.
(40) Freeland, J. W.; Chakhalian, J.; Boris, A. V.; Tonnerre, J.-M.; Kavich, J. J.; Yordanov, P.; Grenier, S.; Zschack, P.; Karapetrova, E.; Popovich, P.; Lee, H. N.; Keimer, B. *Phys. Rev. B* **2010**, *81*, 094414.
(41) Nanda, B. R. K.; Satpathy, S.; Springborg, M. S. *Phys. Rev. Lett.* **2007**, *98*, 216804.